Strengthening of steel member using unbonded CFRP laminates

Fengky Satria Yoresta[1,*], *Ryotaro* Maruta[1], *Genki* Mieda[1], and *Yukihiro* Matsumoto[1]

[1]Department of Architecture and Civil Engineering, Toyohashi University of Technology, 441-8580 Toyohashi, Japan

Abstract. Excellent mechanical and physical properties make carbon fiber reinforced polymer (CFRP) the best options for repair, retrofit, and rehabilitation of civil engineering structures. A great success on application of this material in reinforced concrete (RC) structures has attracted much attention from many researchers to develop it in combination with steel. The number of studies on the use of CFRP composites for strengthening steel structures has still been limited and needs to be more explored. To date, the research in this field has mainly focused on CFRP strengthening with adhesively-bonded technique. This paper reports an experimental study to investigate the performance of slender axial compression steel members partially strengthened with unbonded CFRP composites. The requirements for stiffener to prevent buckling occurred in stiffening region are derived from structural equilibrium conditions. Vacuum-assisted Resin Transfer Molding (VaRTM) method is adopted to form CFRP laminates in the strengthened specimens. Totally eight small scale specimens are tested, and it is clear from the test that improvement in load-carrying capacity can be achieved by using CFRP.

1 Introduction

The use of carbon fiber reinforced polymer (CFRP) for repairing and strengthening of reinforced concrete (RC) structures has shown a great success. CFRP is proven to be able to improve flexural strength, shear strength, confinement, and/or fatigue performance of RC components. This is inseparable from excellent properties of this material such as high strength-to-weight ratio, lightweight, excellent fatigue properties, and excellent resistance to corrosion [1-3]. It is also easy to handle, very flexible, and can be applied to any shape of structures. Following to concrete structures, nowadays, the use of CFRP in strengthening of steel structures is becoming popular and attracts much attention [4-5].

Recent studies on the use of CFRP for strengthening steel structures have been conducted by many researchers on several issues. Some of them including flexural strengthening of steel beam [6-9, 2], fatigue strengthening [10-14], confinement short steel columns [15-18], and strengthening of slender steel columns for buckling control [19-22].

However, the method of strengthening steel members in nearly all previous studies is conducted by directly sticking CFRP to steel surface (adhesively-bonded). Although the CFRP adhesively-bonded technique, in many laboratory experiments, has proven effective for improving the load-carrying performance of steel members, this method is considered to be quite troublesome in application because it requires appropriate steel surface treatment before applying CFRP in order to attain acceptable bond between CFRP and steel surface. Different methods of surface treatment will effect on bonding strength [23]. Three main properties of the treated surface are needed to characterize the bonding capacity, i.e. surface energy, surface chemical composition, and surface roughness/topography [4], and of course, all of these properties cannot be easily measured on-site for rehabilitation of existing steel structures.

The use of unbonded CFRP method for strengthening steel structures has not been adequately explored to date. However, the potential use of this technique has been shown in a few studies conducted, such as the ones seen in Ghafoori et al. [24], Ye et al. [25], and Hosseini et al. [26].

In this paper, the unbonded CFRP strengthening method for improving buckling resistance and compressive performance of steel members is proposed. The proposed method is intended to eliminate the troublesome stages of surface treatment in the bonded reinforcement technique so that the rehabilitation of existing steel structures becomes more efficient. In order to achieve this goal, small-scale laboratory tests are conducted on slender steel members by varying its configuration. The results are compared with non-strengthened members to confirm the effectiveness of this method.

2 Theoretical Equations for Stiffener

In this section, stiffening requirements are developed by considering the structural model shown in Fig. 1. In this model, two ends of the member are free to rotate. The

* Corresponding author: syfengky@gmail.com

member is partially stiffened with CFRP in the middle of the span, and the unbonded condition is represented by space between steel and stiffener. The presence of CFRP is intended to inhibit the bending deformation (buckling) caused by compressive force so that the compressive strength of the member increases.

Considering the model in Fig.1, the buckling inhibition is achieved by changing from Fig. 1a to Fig. 1b, and finally reaching Fig. 1c. In order for the plastic hinge to occur at non-stiffening part (at the end of CFRP stiffener) (Fig.1d), the moment M_1 must be larger than M_2, so that the required stiffness can be evaluated by Eq. (1). Other than that, since the stiffening member is in state of three-point bending, the reaction force Q applies when the stiffened member comes into contact with the center of stiffener, so the required strength can be calculated by Eq. (2). Furthermore, in order to resist the reaction force Q, it is also necessary to consider the bearing strength of the stiffening member. The required circumferential strength is then evaluated by Eq. (3).

3 Experimental Program

This experimental program consisted of testing eight specimens under compressive loading to investigate the buckling response of the steel members after wrapping with CFRP laminates. The specimens are divided into two main groups based on slenderness ratio (λ), namely Group 1 with slenderness ratio 70 and Group 2 with 95. Each group possesses two kinds of CFRP stiffening length (L_2) with the thickness of CFRP (t), also bare steel as control un-strengthened specimen. In order to achieve free end rotation, ends of the steel members are cut and formed like a knife blade (Fig.2a). Table 1 summarizes details of specimens used in this experiment.

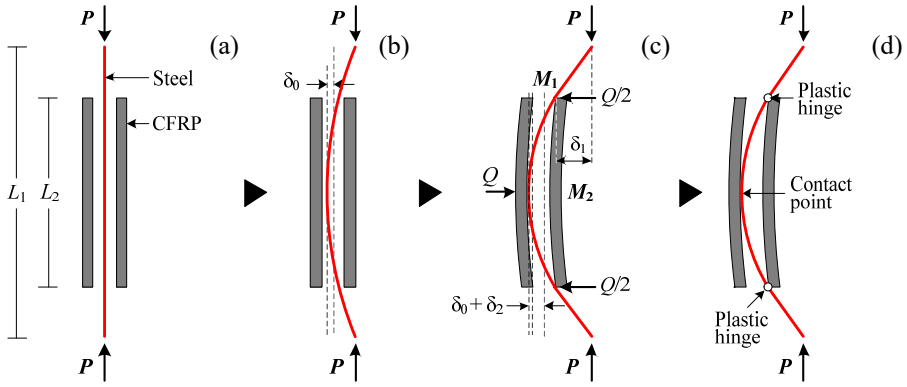

Fig. 1. Specimen model: (a) initial position, (b) applied loading, (c) overall buckling, and (d) location of plastic hinge & contact point.

$$P\left(1+\frac{\delta_0}{\delta_2}\right)=1.5f_{sc}A_s\left(1+\frac{\delta_0}{\delta_2}\right)<\left(\frac{L_2^{\,2}}{12E_{CF}I_{CF}}+\frac{2}{G_{CF}A_{CF}}\right)^{-1} \tag{1}$$

$$1.5f_{sc}A_s\left(\delta_0+\delta_{2,CF,ul}\right)<\frac{1}{4}Q_{CF,ul}L_2 \tag{2}$$

$$f_{CF,ul,T}>\frac{8Q_{CF,ul}}{\pi t_{CF}D} \tag{3}$$

Descriptions:

L_1	is total length of steel bar
L_2	is length of stiffener (CFRP)
δ_0	is gap between steel and CFRP
δ_1, δ_2	is deformation of steel and CFRP due to buckling, respectively
$\delta_{2,CF,ul}$	is allowable deformation of CFRP
f_{sc}	is allowable compressive stress of the member for sustainable load (AIJ recommendation)
$f_{CF,ul,T}$	is circumferential strength of CFRP
A_s, A_{CF}	is sectional area of steel and CFRP, respectively
E_{CF}, G_{CF}	is elastic and shear modulus of CFRP restrainer, respectively
I_{CF}, Z_{CF}	is moment inertia and section modulus of CFRP, respectively
$Q_{CF,ul}$	is reaction force at breaking of CFRP (determined by shear and bending failure)
t_{CF}	is CFRP thickness
D	is diameter of steel bar

Round steel bar Grade G3101 SS400 (JIS Standard) with 32 mm diameter is used in this experiment. The type of CFRP used in the test is bidirectional high strength cloth (BT70-20, [0/90] orientation angel of fiber) produced by Toray Industries, Inc. Obtained from the manufacturer, the properties of this material are as follows: tensile strength is 2.9 GPa, elastic modulus is 230 GPa, density is 1.8 g/cm^3, and sheet thickness is 0.112 mm. The epoxy resin used is obtained from different manufacturer and possess features that of ultra-low viscosity and high strength.

Vacuum-assisted Resin Transfer Molding (VaRTM) technique is adopted to make unbonded CFRP stiffener for all strengthened specimens. This technique is intended to minimize gap between steel and CFRP. In order not to bond with carbon fiber, steel bar that has been cut in decided length is firstly covered with a layer of peel ply (as unbonded material) after its surface is wiped with acetone. The carbon fiber sheet is then wrapped up following the peel ply until it reaches the number of lamination as designed. After that, another peel ply, infusion mesh (resin media), infusion spiral tube, a bagging film (with firmly gum tape connection), and PVC hose (for resin feed line) are installed sequentially before the resin impregnation process is conducted by way of vacuum suction (Fig.2b). Once the vacuuming process is complete, the specimens are then cured for a week.

After completing the manufacturing process, all specimens are then monotonically loaded using a 2000 kN Maekawa testing machine. A load cell built-in within the testing machine is used to measure the applied load, and six transducers (LVDTs) are mounted around the specimens to measure reliable out-of-plane deformation. Fig.3 shows the test setup of the specimens.

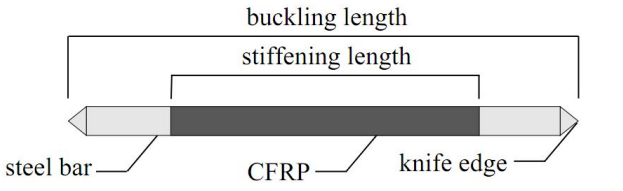

(a)

(b)

Fig. 2. Tested specimen: (a) specimen configuration, (b) molding process

4 Results and Discussions

Table 1 shows the maximum loads (P_{max}), maximum stress (σ_{max}), and stiffening effect (η) achieved for each specimen. The maximum load is normalized by the yield capacity, and the stiffening effect is expressed in percentage and denoted by "+" sign to show the increasing value from that of the control specimen. The load versus out-of-plane deformation response at steel near the edge of CFRP stiffener is then shown in Fig.4a and Fig.4b, and the failure modes for selected specimens are shown in Fig. 5.

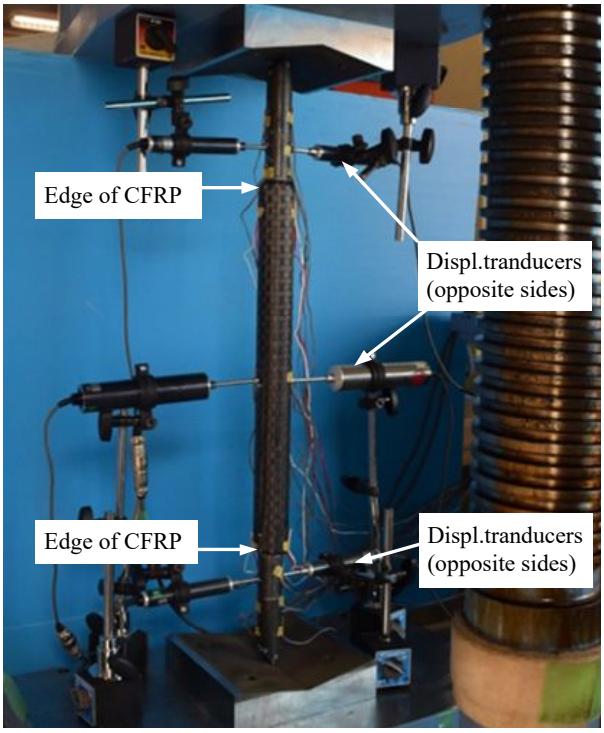

Fig. 3. Specimen test setup

From Table 1, all specimens buckle before reaching yield point as designed. Buckling occurs at varying loads, ranging from 155 to 250 kN. Two control specimens (specimen 560-NS and 760-NS), as generally predicted, buckle in the first buckling mode of pin-ended slender column (Fig. 5a and Fig. 5c) at around 80% and 60% of the yield load, respectively. Taking control specimens as reference, the buckling in all CFRP-strengthened specimens does not occur along the stiffening part, but it lies in steel near the end of CFRP (Fig. 5b and Fig. 5d). Furthermore, observing the failure modes of the specimens also reveals that there is no crushing in CFRP during the test.

All of strengthened specimens in each group possess the value of maximum stress larger than the un-strengthened steel. This is proving, therefore, that the existence of CFRP gives better effects in enhancing axial compressive strength. For example, the strength increase reaches 18.3% and 49.9%, respectively, in specimen 760-360 and 760-460. However, the variation values in stiffening effect are also confirmed. Specimen 560-260-2 which is 5.85 mm in thickness of CFRP has a strength increase no more than 10%, while specimen 560-260-1, with lower thickness of CFRP, increases more than 15%. The same case can also be found in specimen 560-340-1 and 560-340-2. The reason behind this could be because of specimen imperfection. The stiffener molding process does not perfectly form CFRP laminates in a circular shape.

Table 1. Summary of specimen and test results.

Specimen	Buckling length (mm)	L_2 (mm)	t (mm)	P_{max} / P_y	σ_{max} (MPa)	η (%)	Failure mode
Group 1							
560-NS	560	-	-	0.81	266	-	Global buckling (GB)
560-260-1	560	260	5.30	0.94	309	+16.4	GB on steel near the edge of CFRP
560-260-2	560	260	5.85	0.86	283	+6.3	GB on steel near the edge of CFRP
560-340-1	560	340	5.43	0.95	310	+16.8	GB on steel near the edge of CFRP
560-340-2	560	340	6.02	0.89	290	+9.0	GB on steel near the edge of CFRP
Group 2							
760-NS	760	-	-	0.59	192	-	GB
760-360	760	360	6.04	0.69	227	+18.3	GB on steel near the edge of CFRP
760-460	760	460	6.97	0.88	288	+49.9	GB on steel near the edge of CFRP

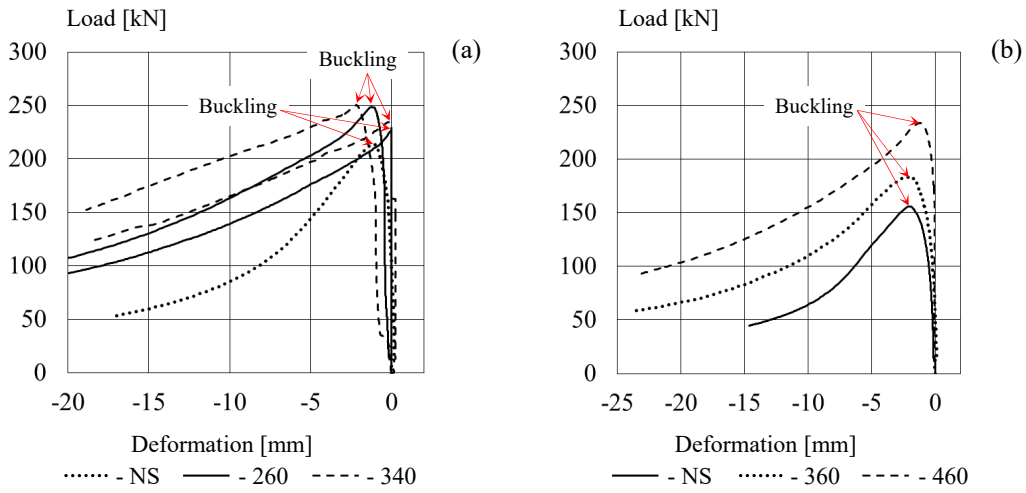

Fig. 4. Load-deflection curve: (a) specimens Group 1, and (b) specimens Group 2.

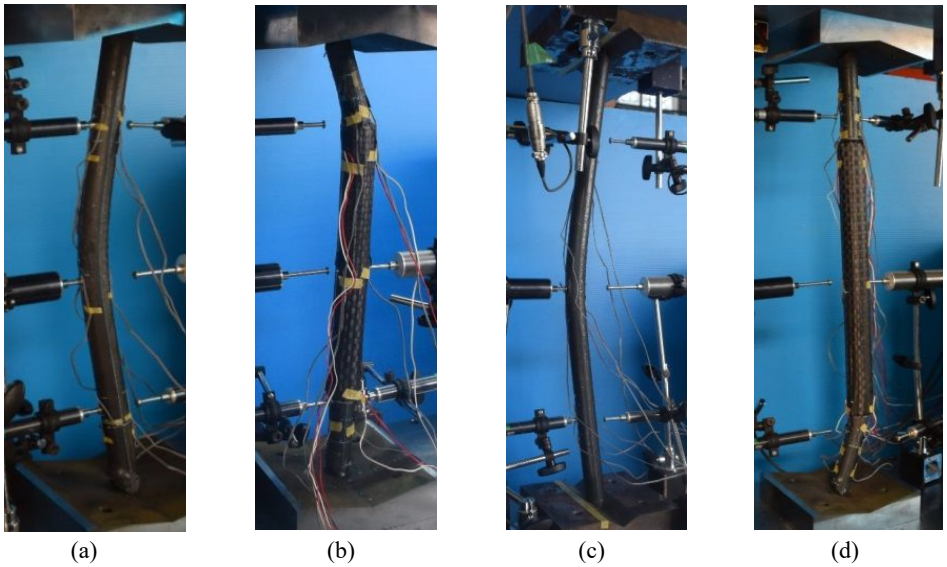

Fig. 5. Failure modes: (a) specimen 560-NS, (b) specimen 560-340, (c) specimen 760-NS, and (d) specimen 760-460.

5 Summary and Conclusions

Unbonded CFRP strengthening method for slender axial steel members has been investigated in this experiment. From structural equilibrium conditions, the expressions for stiffening requirements are then introduced. The experimental program involves small-scale specimens that are different in length, length of stiffener, and stiffener thickness. Even though the testing results show a presence of variation, it can be confirmed that this method can be used to control the buckling response and increase the compressive strength of steel members. Furthermore, research involving many specimens and variables is needed in order to achieve more comprehensive results.

References

1. X.L. Zhao, L. Zhang, Eng. Struct. **29**, 1808-1823 (2007)
2. T.W. Siwowski, P. Siwowska, Compos. Part B **149**, 12-21 (2018)
3. B.H. Osman, E. Wu, B. Ji, S.S. Abdulhameed, Housing and Build. National Res. Center **14**, 29-36 (2018)
4. J.G. Teng, T. Yu, D. Fernando, J. Constr. Steel Res. **78**, 131-143 (2012)
5. M.R. Ghaemdoust, K. Narmashiri, O. Yousefi, Constr. Build. Mat. **126**, 1002-1011 (2016)
6. D. Linghoff, M. Al-Emrani, R. Kliger, Compos. Part B **41**, 509-515 (2010)
7. K. Narmashiri, N.H.R. Sulong, M.Z. Jumaat, Constr. Build. Mat. **30**, 1-9 (2012)
8. M.H. Kabir, S. Fawzia, T.H.T. Chan, J.C.P.H. Gamage, J.B. Bai, Eng. Struct. **113**, 160-173 (2016)
9. M.J. Altaee, L.S. Cunningham, M. Gillie, J. Constr. Steel Res. **138**, 750-760 (2017)
10. M. Bocciarelli, P. Colombi, G. Fava, C. Poggi, Compos. Struct. **87**, 334-343 (2009)
11. Y.J. Kim, K.A. Harries, Eng. Struct. **33**, 1491-1502 (2011)
12. Q.Q. Yu, T. Chen, X.L. Gu, X.L. Zhao, Z.G. Xiao, Thin-Walled Struct. **69**, 10-17 (2013)
13. Z.Y. Wang, Q.Y. Wang, L. Li, N. Zhang, Thin-Walled Struct. **115**, 176-187 (2017)
14. E. Lepretre, S. Chataigner, L. Dieng, L. Gaillet, Constr. Build. Mat. **174**, 421-432 (2018)
15. M.R. Bambach, H.H. Jama, M. Elchalakani, Thin-Walled Struct. **47**, 1112-1121 (2009)
16. J. Haedir, X.L. Zhao, J. Constr. Steel Res. **67**, 497-509 (2011)
17. M. Karimian, K. Narmashiri, M. Shahraki, O. Yousefi, J. Constr. Steel Res. **138**, 555-564 (2017)
18. A.B.B. Abu-Sena, M. Said, M.A. Zaki, M. Dokmak, Constr. Build. Mat. **205**, 306-320 (2019)
19. E.Y. Sayed-Ahmed, A.A. Shaat, E.A. Abdallah, J. Compos. Constr. **22**, 1-14 (2018)
20. A. Ritchie, A. Fam, C. MacDougall, J. Compos. Constr. **19**, 1-11 (2015)
21. X.Y. Gao, T. Balendra, C.G. Ko, Eng. Struct. **46**, 547-556 (2013)
22. A. Shaat, A.Z. Fam, J. Compos. Constr. **13**, 2-12 (2009)
23. J.G. Teng, D. Fernando, T. Yu, X.L. Zhao, Proc. The 5th CICE Conf. **2**, (2010)
24. E. Ghafoori, M. Motavalli, J. Botsis, A. Herwig, M. Galli, Intl. J. Fatigue **44**, 303-315 (2012)
25. H. Ye, C. Li, S. Pei, T. Ummenhofer, H. Qu, J. Bridge Eng. **23**, 1-12 (2018)
26. A. Hosseini, E. Ghafoori, M. Motavalli, A. Nussbaumer, X.L. Zhao, R. Al-Mahaidi, G. Terrasi, Eng. Struct. **181**, 550-561 (2019)